Eur. Phys. J. Special Topics **204**, 85-101 (2012)

DOI: 10.1140/epjst/e2012-01554-x

THE EUROPEAN PHYSICAL JOURNAL SPECIAL TOPICS

Review

Probing single cells using flow in microfluidic devices

D. Qi[a], D.J. Hoelzle[a], and A.C. Rowat[b]

Department of Integrative Biology and Physiology, University of California, Los Angeles
610 Charles E. Young Drive, Los Angeles, CA 90095, USA

Received 23 December 2011 / Received in final form 22 February 2012
Published online 17 April 2012

Abstract. Enabling fluids to be manipulated on the micron-scale, microfluidic technologies have facilitated major advances in how we study cells. In this review, we highlight key developments in how flow in microfluidic devices is exploited to investigate the behavior of individual cells, from trapping and positioning single cells to probing cell deformability. Exploiting the properties of fluids and flow patterns in microchannels makes it possible to study large populations of single cells at micron-length scales with increased throughput and efficiency.

1 Introduction

Flow is central to life: the transit of red blood cells through capillaries is critical for gas exchange; the spread of white blood cells is essential for immune function; stem cells, metastatic cancer cells, as well as drugs travel through the bloodstream, and their spread is critical in biomedical contexts ranging from stem cell therapeutics to cancer progression to drug delivery. Understanding how cells behave during flow and are distributed throughout the bodily network of arteries, veins, and capillaries has motivated numerous studies during the past decades. For example, *in vivo* imaging of red blood cells reveals how they adapt an inverted, umbrella-shape during passage through narrow capillaries [1]; fabricated junctions of capillary tubes are used to investigate the flow of cells through branching networks [2]; bulk filtration is used to probe the effect of cell stiffness on the ability of cells to deform through the tiny constrictions of a porous membrane, providing insight into the mechanisms of increased cell stiffness that can result in occlusion and retention in capillaries [3]. Flow is also central to many common procedures in biological research: cells are transferred from petri dish to test tube using pipettes to manipulate the fluid in which they are suspended; cellular contents are routinely separated with centrifugal forces; DNA is ordered by size using electrophoresis to filter the biopolymer solution through a porous gel. While these techniques provide insight into biological systems, analysis of gene or protein expression levels typically requires material from thousands to millions of individual cells (microarrays or western blots), and operates on the scale of microliters to milliliters; this inherently limits the ability to study femoliter-volume

[a] Equal contribution.
[b] e-mail: rowat@ucla.edu

single cells. By dispersing individual cells into a streamline of fluid, flow cytometry enables single cells to be interrogated one-by-one using light; this enables quantitative measurements of protein levels, DNA content, as well as cell size at rapid rates of up to 10^5 cells s^{-1}. Flow cytometry is thus a powerful tool that provides insight into the distribution and variability among a population of individual cells at a particular instant in time. Together these flow-based studies and techniques have advanced our biochemical understanding of cells, while probing the force-deformation response of small numbers of 10–100 single cells provides insights into cell mechanical properties. Yet there are certain questions that these methods cannot address: How do individual cells respond to chemical gradients? What is the dynamic response among a population of single cells to oscillating stimuli? What is the variability in cell mechanical properties among a population of single cells?

With the ability to manipulate fluids and cells on the *micron*-scale, microfluidic devices make it possible to address such questions and measure the behavior of single cells. The establishment of this technology was catalyzed by the development of soft lithography fabrication techniques [4–6], enabling major advances in many fields including a new class of tools to study individual cells. Microfluidic devices can be easily and inexpensively fabricated; these devices have channels with dimensions similar to the scale of individual cells and therefore make it possible to manipulate, spatially position, and deform single cells. Since fabrication is inexpensive, devices can be tailored to a specific analysis; moreover, designs can be efficiently iterated to improve the experiment with little investment. In contrast to many conventional methods, microfluidic technologies offer powerful advantages in enabling routine studies to be scaled down significantly in volume. The capability to investigate single cells, measure their gene and protein expression levels, as well as their physical properties, enables data to be compiled for an entire population, revealing rich phenotypic variability as well as subpopulations of cells that would otherwise remain hidden in bulk population studies. The ability to entrap single cells and perform experiments with picoliters of reagents also provides major advances in biotechnology: biochemical reactions can be performed with order-of-magnitude reductions in volume and with unprecedented throughput. Moreover, the ability to trap single cells has profound biomedical and clinical implications: single circulating tumor cells (CTCs) can be isolated and subjected to detailed characterization, and drug response can be monitored at the level of single cells over time.

In this review, we highlight two major themes in using micron-scale fluid flows to probe cells: flow is exploited 1) to spatially position cells at defined locations, for example to investigate their response to local chemical environments, and 2) to subject cells to physical forces in order to probe their deformability. To begin, we provide an introduction to basic concepts in microfluidics for the general reader who is not familiar with this methodology, including a brief description of device fabrication and the fluid dynamics within microfluidic channels.

2 Basics of microfluidics for cell studies

2.1 Fabricating microfluidic devices

Microfluidic devices can be easily and consistently fabricated using soft lithography, a printing technique with a similar concept to silk screening or the pre-digital process of photography. The end goal is to pattern a network of micron-scale channels with a defined height onto a substrate (Fig. 1.1); typically a silicon wafer is used, borrowing techniques developed for the semi-conductor industry. To generate device designs, standard CAD software, such as AutoCAD, is widely used. The design is printed

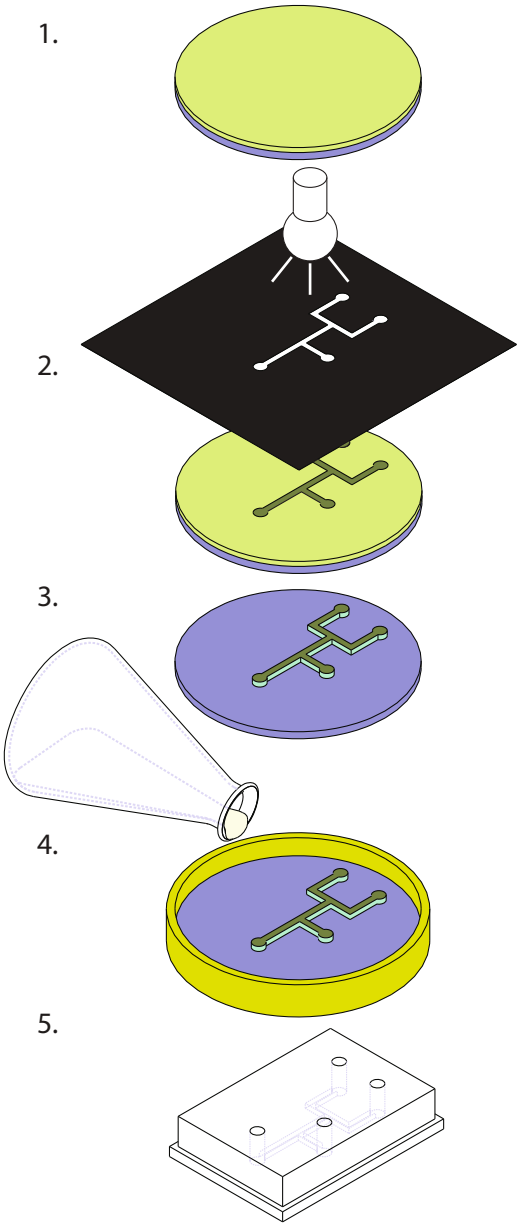

Fig. 1. Overview of microfluidic device fabrication by soft lithography. 1) Photoresist is spincoated onto a substrate to a desired thickness that sets the channel height. 2) A mask provides a template for the channels; it is placed above the photoresist; upon exposure to UV light, photoresist molecules below the transparent channel regions are crosslinked. 3) Uncrosslinked photoresist is removed using a developer solution to reveal a raised relief of the microfluidic channels. 4) Elastomer (typically PDMS) is poured onto the mold, degassed, and baked. 5) The solid PDMS device is cut from the mold, holes are excised to enable external flow control to interface with the channels, and the device is bonded to a glass substrate.

onto a mask, which provides the template for the channels. For channels down to approximately 5 μm width, designs may be inexpensively printed onto a transparency at a high-resolution of 20,000 dpi (Fig. 1.2); smaller features down to 0.75 μm can be achieved by printing on a quartz mask. The channel height is set by the thickness of the photoresist, a UV-curable resin that is used to define the microfluidic channels: in the cleanroom, photoresist is spincoated onto a silicon wafer to a defined height determined by the viscosity of the photoresist and the spin speed; this facilitates a range of channel heights from 1 to 100 μm. Next, the mask is placed atop the photoresist: channel regions are transparent, so that UV exposure causes the molecules of photoresist to crosslink in the channel regions; the unexposed photoresist can be rinsed away in the developer solvent to create a master mold (Fig. 1.3). The channels form a negative mold over which liquid polymer and cross-linking agents are poured (Fig. 1.4); baking crosslinks the polymers and results in an elastomer that is imprinted with an inverted, raised-relief of the channels. The elastomer of choice is polydimethylsiloxane (PDMS): it is transparent, flexible (Young's modulus 10^5–10^6 Pa), gas permeable, and silicon-based, therefore it can be covalently bonded to glass substrates via plasma treatment. It can also be bonded to itself, which is valuable for creating multilayer stacks of PDMS. Holes are excised using a needle or biopsy punch (Fig. 1.5), enabling tubing to be inserted into the device, so that flow through microchannels can be externally controlled via gravity, pressurized air or syringe pumps. The entire fabrication process requires only a few hours from spincoating to bonding, and masters can be reused to mold fresh devices multiple times. The cost of raw materials per device is less than one dollar.

PDMS devices offer great flexibility in design and fabrication: devices can be integrated with electronics for detection or activation [7–9]; since PDMS is optically transparent, devices can be interfaced with optics for myriad applications ranging from fluorescence detection [9] to cell stretching by optical traps [10]. While peripheral equipment can easily interface with PDMS devices, a great advantage of PDMS fabrication is that microfluidic channels can themselves be integrated components in a single device. For example, pressurized lines can carry gaseous species that permeate the PDMS walls to spike a sample volume [11]; a channel injected with molten solder becomes an integrated electrode upon cooling that easily interfaces with external electronics [12]. Such integrated electrodes can be energized to produce an electric field gradient across the width of the flow channel that can be applied for dielectrophoretic manipulation and sorting of cells in water-in-oil emulsion droplets [9]. Valves can also be integrated into a flow channel by fabricating a pressurized air channel that lies beneath and intersects the flow channel; activating the air channel causes the flexible PDMS membrane to deflect into the flow channel, thereby blocking the majority of fluid flow [13,14]. Valves can also be fabricated in a single layer, with the pressurized control channel fabricated less than 10 μm apart from the flow channel; the flexible PDMS wall deflects when pressurized and flow is diverted [15]. Taken together, these design and fabrication capabilities make it possible to generate and manipulate flow on micron length scales. The resulting flow on such small scales has some interesting and unusual properties that can be exploited to probe single cells in ways that were previously not possible.

2.2 Brief theoretical description of flow in microfluidic devices

The theoretical underpinnings of flow in microfluidic devices are thoroughly covered in many excellent reviews [16–18]. Here we provide a brief overview for the general reader. In most microfluidic devices, the flow is laminar and has certain characteristics that can be exploited in experimental design.

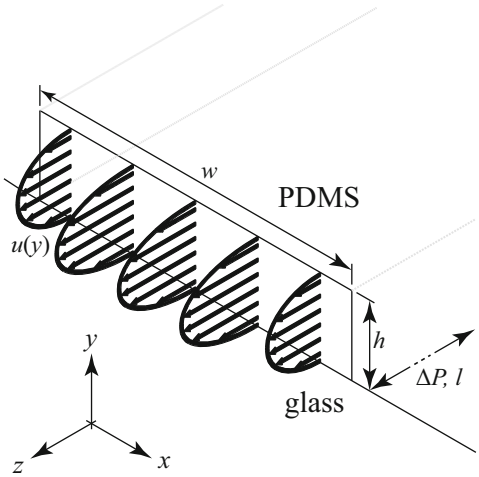

Fig. 2. Hagen-Poiseuille flow in a microfluidic channel with a rectangular cross-section. The flow velocity profile is assumed to be a function of the position in the y direction.

2.2.1 Laminar flow

The small scale of cells and microfluidic channels means that viscous forces generally dominate inertial forces; mixing occurs only by diffusion. The relationship between inertial to viscous forces is described by the dimensionless Reynolds number, $\mathrm{Re} = \frac{Lv\rho}{\eta}$, where L is the characteristic length scale [m], ρ is the density [kg/m^3], v is the average velocity [m/s], and η is the dynamic viscosity [Pa $\cdot$ s] of the fluid. Given that the channel width, or hydraulic diameter of a cell, is $L \backsim 10^{-6}$ m, typically $\mathrm{Re} = 1$–100. In the *laminar* flow regime, streamlines are smooth; the etymology of 'lamina', meaning thin plate, provides a nice depiction of the sheaths of fluid flowing past each other. By contrast, turbulent flow is characterized by higher Reynolds numbers, $\mathrm{Re} > 10^3$; here inertial forces dominate and flow patterns exhibit instabilities such as vortices and eddies. The laminar flow properties of microfluidic devices can be exploited for biological experiments: for example, the effect of temperature on *Drosophila* embryo development is elegantly probed by positioning the embryo across two streamlines of fluids that each have different temperatures, $\Delta T = 7$–$10°$C; in the laminar flow regime, these fluids mix only by diffusion and thereby enable investigations of the embryo's response to different temperatures [19].

2.2.2 Hagen-Poisseuille equation

Given these laminar flow properties, flow through the typical rectangular channels of a microfluidic device can be described by Hagen-Poiseuille equation. The basic assumptions are: flow is laminar; fluid is incompressible ($\nabla \cdot \mathbf{u} = 0$); flow does not change over time (steady-state, $\frac{\partial \mathbf{u}}{\partial t} = 0$); no slip at wall ($u = 0$ at $h, w = 0$). With these assumptions, the relationship between the pressure drop and flow rates through microfluidic channels over length, l, can be described by the Hagen-Poisseuille equation (Fig. 2). Derived from Navier–Stokes equations, the Hagen-Poisseuille equation describes the relationship between pressure drop, flow velocity, and channel dimensions for a pipe with a circular cross-section. Microfluidic channels are typically not round, but rectangular as a result of the manufacturing process; the parabolic flow

velocity distribution across the height of a rectangular channel for the ideal case where $h \ll w$ is described as:

$$u(y) = \frac{\Delta P}{2\eta l} y(h - y).$$

The average volumetric flow rate, Q [m^3/s] can be obtained by integrating over the channel's cross-section,

$$Q \backsim \int_{-w/2}^{w/2} \int_0^h u dy dx \backsim \frac{\Delta P}{l} \frac{h^3 w}{12\eta} \tag{1}$$

where $\frac{12\eta l}{h^3 w}$ is the hydrodynamic resistance. Considering fluidic circuits analogous to electrical circuits, this resistance can also be described in terms of Ohm's law, $V = IR$, where $V \backsim \Delta P$, $Q \backsim I$, and R is the (hydrodynamic) resistance.

3 Using flow to place cells

The beauty of fluid flow is that it can be controlled and exploited to achieve precise, spontaneous placement of hundreds to millions of cells, which can simplify both data collection and analysis. Precision control can also be achieved by interfacing the devices with active features for cell manipulation. Cells are typically suspended in a carrier fluid, such as an aqueous medium, whose flow rate determines the speed at which cells are carried through the micron-scale channels, and facilitates rapid characterization of cells at rates of up to thousands per second. Microfluidic assays thus typically require significantly less labor and can be easily scaled up, making these methods also amenable for experiments with milliliter volumes of fluids, such as required for clinical applications. Moreover, devices can run for hours with minimal human intervention [20]; such autonomy and consistency results in limited opportunities for human error and measurement variability.

3.1 Positioning cells in a microchannel by flow

Exploiting flow properties, cells can be positioned in the fluid stream across the width of a microfluidic channel. Such techniques are valuable for aligning cells for downstream processing and separating cells based on their physical properties.

3.1.1 Flow focusing

One simple way to position cells in the middle of a channel is to focus two opposite streamlines into the flow emerging from a single channel. A similar principle is used in flow cytometry to position cells in a single line as they flow past a laser; this enables the fluorescence levels of individual cells to be quantitatively measured. In microfluidic devices, centering cells laterally within a flow channel is valuable when the cell needs to be positioned for downstream processing, such as entrapment within an emulsion droplet [9,36]. The ability to center cells in a flow stream also has practical applications for integrated microfluidic devices: For example, cells positioned in the middle of a channel can be subject to the well-controlled external forces of an optical trap, or chemical or electric field gradient. With such established tools integrated into a microfluidic network, the rates of single cell characterization increase significantly and minimize operator intervention. For example, the automated optical

'Cell Stretcher' device consists of two diametrically opposed laser beams that trap and stretch individual cells that flow through the channel of a microfluidic device [10,37]; the incident laser light creates a surface force on the cell and induces cellular deformation. Relative to other methods to probe cell mechanical properties, conveying the cells using flow results in increased characterization rates of up to 1 cell per minute. The method reveals distinct differences between malignant and benign cells from oral cancer patients [38], including various other model cell lines: red blood cells [37,39]; fibroblasts [37], neurons and glial cells [40].

The opposite of flow focusing – where a cell of interest is forced to the channel wall as opposed to the center – can be used to separate rare leukocyte cells from whole blood. Blood cells flowed at high density (45 vol%) are subject to 'margination' forces, which result from cell–cell interactions between red blood cells and subsequent displacement of the larger leukocytes to the channel wall [41]. Tangential side channels, analogous to a highway off-ramp, are used to collect rare leukocyte cells, and achieve over 30-fold enrichment.

3.1.2 Ordering cells using inertial flow

While flow in microfluidic channels is typically in a Stokes flow regime, higher flow rates can be used to exploit the forces generated by inertial flow to achieve spatial positioning of cells: a fluid shear gradient drives cells laterally towards the channel walls, while competing wall-effect forces drive particles towards the channel center; the balance between these two opposing forces determines the equilibrium lateral position of a cell or particle within a microchannel. The magnitude of these forces acting on the cell body depends on the size of the cell, which determines its lateral position within the flow channel [24–33]. The deformability of the cell also plays a role in its equilibrium lateral position, due to the forces acting on the interface between the cell and the surrounding fluid. Inertial ordering can thus be used to distinguish between cells types based on their physical properties via their lateral equilibrium position. For example, cells of different sizes, such as bacteria cells (*Escherichia coli*, diameter $\backsim$ 1–2 μm) and human red blood cells (diameter $\backsim$ 6–8 μm), occupy distinct lateral positions within a channel [28]. In addition, the method can be used to separate and enrich subpopulations of cells: by flowing cells past an adjacent open chamber (Fig. 3), wall-effect forces are momentarily removed and the resulting force imbalance displaces cells from their equilibrium position. In this way, larger cells such as cancer cells, can be enriched from a milliliter-volume blood sample without any additional labeling of cells, such as fluorescent molecules that target specific surface proteins [24]. Exploiting this inertial lift phenomenon while manipulating channel geometry can further enhance bioparticle separation. For example, particle equilibrium positions in curved or spiral microchannels depends on the balance of inertial lift and drag forces which result from fluid vortices across the channel cross-sections [26,30]. The ratio of these two forces depends on the particle size, and can thus be exploited to separate a mixture of particles of different sizes with efficiencies of up to 80% [30].

3.1.3 Spatially positioning cells using structures

Flow can be used to rapidly position cells at a predefined location in a microfluidic device by carrying the cells into fabricated structures, akin to trapping cells in cages. By manipulating the design of these structures, single cells, pairs of cells, and lineages of cells can be spatially organized; this ability is valuable across a range of fields ranging from epigenetics to stem cell biology. Typically cells are flowed *en masse* over

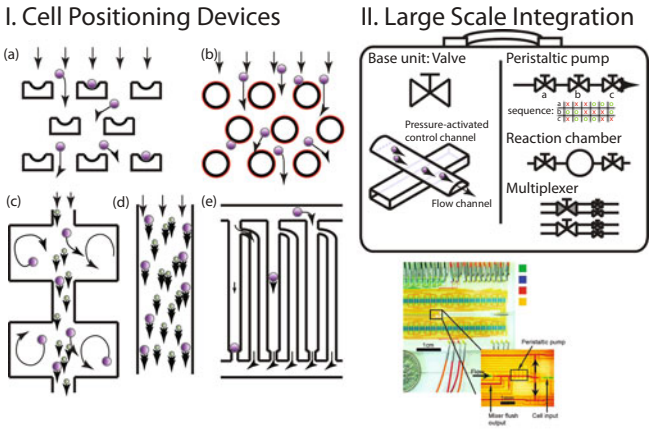

Fig. 3. Methods to position cells using flow in microfluidic devices. I. Cell positioning devices use flow to position cells for subsequent analysis: (a) trapping cells by flowing them into traps [21,22]; (b) adhering cells to structured posts functionalized with antibodies [23]; (c) laterally positioning and separating cells based on their size using shear-gradient lift forces [24]; (d) separating cells based on their size and relative deformability using inertial forces generated at high flow rates [25–33]; (e) positioning single cells and their lineages in constricted channels of a device whose design exploits the changes in resistance that occur when a single cell plugs a channel [34]. Cells are represented by purple spheres, functionalized surfaces are denoted by red lines. **II. Microfluidic large-scale integration** uses valves as a base unit to construct complex digital flow networks. Valves can be combined to perform a set of basic functions, some of which are shown in the toolbox; these functions can be integrated into a system to perform complex cell and chemical manipulations. Some basic functions are: *in situ* pumping of fluid flows using three valves in series that are actuated in the time sequence shown (x = valve closed, o = valve open); confined reactions can be performed in a reaction chamber by closing valves on either side of channel; multiplexing enables control of thousands of individual compartments with a few hundred valves [13]. Complex microfluidic large scale-integration image has been adapted with permission from [35]. Copyright 2007 American Chemical Society.

an array of traps with filling efficiencies that are described a Poisson distribution (Fig. 3).

3.1.4 Positioning cells by designed structures

The simplest example of trapping cells relies on confining cells in the planar dimension, where the channel height is equivalent or lesser than the cell diameter. Such device geometry is particularly valuable for cells that grow in three dimensions, such as the budding yeast, *Saccharomyces cerevisiae*. Confining the growth of these cells in a planar microfluidic device greatly simplifies the challenge of tracking these cells over time [42]. For example, yeast cells with a diameter of 4–6 μm are conveniently trapped in a 4 μm-high channel; as they grow and divide, multiplying in number, they are forced out into a 8 μm-high fluid reservoir, where they are carried away by the flow [43]. To make tracking individual cells in timelapse experiments more efficient, cells may also be spatially positioned. A simple and elegant way to achieve this is to trap cells in grooved channels, and confine them in a single plane using a porous membrane to prevent growth into the third dimension; this allows for medium exchange over the time course of the experiment [44]. To achieve even greater precision

of single cell placement, cells can be trapped in structures with dimensions similar to single cells. For example, cups or 'yeast jails' on the order of the cell size are used to trap single yeast cells [21], and an array of U-shape trapping structures is used to capture individual human cervical carcinoma (HeLa) cells [22]. With the cells localized in such structures, the medium can easily be changed, enabling studies of the dynamic response of cells to varying environmental conditions [22]. With such exquisite control of single cell placement, these microfluidic devices offering unique advantages over conventional cell culture methods including the ability to monitor single cells while providing constant exchange of fresh nutrients and cell waste for long-term cell culture over days.

The ability to capture single cells is also valuable for trapping specific types of cells out of a heterogeneous population [45]. An excellent example is CTCs: characterizing them can indicate the severity of metastasis. However, there is about 1 CTC for every 10^9 blood cells and trapping these extremely rare cells is a technical challenge. Using microfluidic devices with structures that have a series of posts with dimensions similar to single cells, CTCs have been successfully captured (Fig. 3a); captured cells can be easily retrieved by reversing the flow such that the medium and suspended cells flow in the opposite direction from the back side of the cups. The isolation efficiency of this method is 80%, as measured by testing human breast and colon cell cancer lines [46].

Designed structures can also be used to position two different cell types; this is critical for cell fusion applications. One example is reprogramming somatic cells: this requires fusing a stem and somatic cell together, but conventional methods have poor efficiency and low yield due to limited control of cell–cell interactions. Exploiting the ability to fabricate micron-scale traps for individual cells, an efficient fusion device enables thousands of parallel cell-pairs to be positioned in adjacent traps [47]. Each 'trap' consists of a pillar with curved features on both front and back sides: a shallow cup on the front side, and a deeper cup on the back side. Single cells from sample I are trapped in the shallow sides of the cups; by reversing the flow, one cell of sample I is transferred to the deep side of the cups. Sample II cells are then flowed towards the deep back side of the cups; thus, one cell each of samples I and II are placed in direct contact with each other. Compared to conventional methods of cell-pairing, a two- to ten-fold improvement in fusion yield can be achieved using this device, as well as successful reprogramming of somatic cells [47].

While studies of single cells reveal phenotypic heterogeneity among a clonal population, exactly how cellular behavior is affected by their age and geneaology remains poorly understood. By trapping single cells and spatially confining them as they divide, 'lineage chambers' conveniently entrap a single cell and its progeny, and provide insight into epigenetic phenomenon. One simple method to spatially position single cells and their progeny exploits changes in flow patterns that result from a single cell blocking a channel: the presence of a single cell in the trapping chamber increases the channel's fluidic resistance, and shifts the proportion of fluid flow such that the majority of flow is diverted through adjacent bypass channel (Fig. 3e). In this way, single cells are preferentially trapped, yet can still grow and divide in the confines of the trapping channel; since medium flows slowly and continuously through the trapping channel around the dividing cells. By tracking the cells as they grow and divide, the identity of each cell can be maintained, and complete lineage maps are generated. Such lineage maps provide detailed information about the identity, pedigree, and replicative age of each and every cell. For example, monitoring the growth of yeast cells in the lineage chamber device reveals that patterns of protein expression are shared among cells and their offspring with a timescale that varies for different proteins [34]: protein expression levels of the phosphate transporter, Pho84, are consistent over multiple divisions while bursts in levels of the heat shock

protein, Hsp12, result in protein levels that are maintained only in the most immediate offspring cells.

3.1.5 Cell trapping by surface modification

Cell trapping can be improved by chemically altering the surfaces of microchannels to exploit the unique surface proteins of specific cell types. However, there are typically few interactions between the cells and the walls of a straight channel due to laminar flow properties. To increase the frequency of cell-wall interactions, flow patterns can be modified by fabricating structures that impede flow streams or by increasing channel surface roughness. For example, micropatterned posts that are oriented in an offset array alter the unidirectional flow; functionalizing the posts with antibodies further promotes cell-wall adhesion. Such a method enables cell enrichment and CTC immobilization [24] (Fig. 3b). Cell-wall interactions can also be enhanced by fabricating textured microchannel walls: grooves fabricated with a periodicity of $50\,\mu$m in the channel walls form herringbone structures; structures introduce helical patterns in the laminar flow pattern, and the number of particle-wall collisions is increased [48,49]. Devices with such textured channels achieve capture efficiencies of more than 2.5x compared to the flat-walled device, making this a more efficient method to trap cells; CTCs are successfully isolated from whole blood of patients with prostate and lung cancer with an average capture efficiency of 80% [49].

3.2 Probing cell response to the micron-scale chemical environment

Precise positioning of cells is also exploited to probe cellular response to soluble factors on the micron-scale. With cells trapped in an array, distinct chemical environments can be defined in a microfluidic device by exploiting laminar flow properties [50]. For example, the interface between two flow streams can be transversely shifted by controlling the difference in flow rates using syringe pumps; this manifests as a transverse displacement of the fluid-fluid interface, thereby enabling cells to be subjected to fluctuating or oscillating stimuli on timescales of 10 to 60 seconds. By trapping 10^2–10^3 cells in parallel, the effects of such soluble stimuli can be dynamically applied and cell responses are investigated using fluorescence imaging. For example, cells are seeded in columns of circular wells and exposed to varying temporal profiles of stimuli to elucidate the effects on NFκB transcriptional activation and cell fate [51]. Similar microfluidic devices are used to study the molecular origins of the mating response in yeast cells [52], again benefiting from the ability to expose cells to precisely tuned, linear concentration profiles of pheromone, which remain stable over at least 20 hours. Well-defined, stable chemotactic gradients are also key to systematic investigations of the chemotaxis of motile bacteria and eukaryotic cells [53]. For example, buffer and chemoattractant solutions flow through parallel microchannels, between which horizontal microchannels are used to build chambers that contain stable chemoattractant gradients; cells are seeded in the gradient chambers and their chemotactic responses are investigated. Other devices are also used to create stable, linear concentration gradients [54].

3.3 Trapping cells in droplets

Entrapping cells in droplets of water-in-oil emulsions provides a convenient and efficient method to control the position of large numbers of cells; picoliter to femtoliter

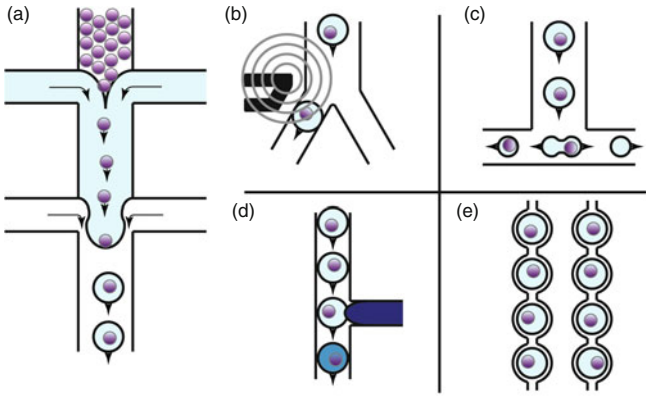

Fig. 4. Drop-based microfluidics. Schematic illustrations showing some basic functions that can be applied to cells trapped in emulsion droplets. (a) Using a flow-focusing device, cells are entrapped in the droplet of an emulsion of two immiscible fluids (oil and an aqueous medium) [36]. Two flow-focusing junctions in series enables cells to be centered in the flow stream prior to encapsulation [9]. The droplet can be used to convey the cell within this tiny picoliter to femtoliter-sized chamber. By exploiting the physical properties of the droplets, cells are subjected to various operations, such as: (b) sorting droplets by dielectrophoresis [9,57]; (c) splitting droplets by shear at a T-junction [58]; (d) injecting droplets with picoliter-volumes of reagents [59]; and (e) trapping droplets [60]. Legend: cells = purple spheres, flow vectors = arrows, aqueous-in-oil droplets = light blue.

droplets are compartments for individual cells that also enable ultra high throughput studies [9,55]. By exploiting the immiscibility of water and oil, individual cells and their secreted compounds can be contained and manipulated. In practice, PDMS microfluidic devices provide a convenient way to generate micron-scale emulsions for single cell studies. Droplets are generated when oil shears the aqueous stream; this can be achieved at a T-junction, or commonly, using a flow-focusing geometry (Fig. 4a) [36]. By tuning the density of cells in the aqueous phase suspension, an average of one cell per drop can be trapped, as described by a Poisson distribution. To beat the Poisson distribution and achieve greater efficiency of single cell trapping, inertial effects can be exploited [56].

Drops of water-in-oil emulsions can be manipulated to perform a range of functions necessary for controlling and detecting biological reactions. For example, drops can be split, merged, and sorted (Figs. 4b-d). Droplets can also be arranged in an array (Fig. 4e): drops are flowed through channels with a series of constrictions; when the applied pressure or flow is above a certain threshold pressure, $\Delta P > \Delta P_{min} \backsim 2\gamma/r$, the drops deform through narrow constrictions and flow through the channels; however, when $\Delta P < \Delta P_{min}$, drops remain stationary. The ability to passively entrap thousands of droplets by their surface tension facilitates time-resolved studies at the single cell level [61]. Since the cell and its secreted content are confined within the droplet, such a method is amenable to single cell studies of enzymatic amplification of protein expression.

Droplets can also be detected using a laser and photomultiplier tube to detect fluorescence intensity as drops flow by the detection region – this is akin to flow cytometry but has the distinct advantage that cells and their contents are self-contained. Drops can also be sorted on demand using the fluorescence signal of the drop or entrapped cell as a sorting criterion [9,57]. The mechanism for sorting droplets is very simple: Drops flow down a bifurcating channel, and will naturally flow down the channel that has the lower hydrodynamic resistance and leads to the 'waste' outlet. In response to

the droplet's fluorescence level, an external force can be generated by energizing the electrode that lies alongside the main flow channel; this creates an electric field gradient across the width of the channel. Since the dielectric constant of water is $\backsim$ 40x larger than oil, the desired aqueous droplets are preferentially diverted into the other arm of the bifurcation, enabling selected droplets to be collected in the 'keep' outlet. This droplet-sorting method can achieve droplet separation up to rates of 2,000 events per second. Such a method for enriching desirable droplets provides a powerful tool for any application where individual cells secrete a compound, or express a surface-displayed protein that is detected using soluble dye amplification methods; for example, hybridomas secreting antibodies, or surface-displayed enzymes expressed in microorganisms. By subjecting the cells to repeated rounds of enrichment, sevenfold increases in enzyme activity are achieved with order-of-magnitude reductions in cost and time compared to conventional assays [9]. In addition to dielectrophoresis, a valve-based sorting mechanism can also be used [15].

3.4 Microfluidic large-scale integration

Flow can also be manipulated using an integrated system of active mechanisms that act in unison, much like microprocessors that use a system of transistors to perform complex computations. Analogous to the transistor in a microprocessor, the base unit in microfluidic large-scale integration systems is the valve. Pioneered by the group of Stephen Quake, networks of valves can direct fluid flows, drive peristaltic pumps, and open and close reaction chambers. These few basic functionalities constitute all the processes needed to create complex devices: 1) three valves in series are sequentially actuated to create a peristaltic pump that can drive *in situ* fluid flows, 2) confined reaction chambers are defined by closing valves at either end of a chamber, and 3) multiplexing valves permits hundreds of channels to be controlled, logically akin to electronics multiplexing. These systems are used to enable discrete movements of single cells between compartments and to perform complex biological analyses within a single compact device. By significantly increasing the automation of such microfluidic devices, both the need for constant operator intervention and process variability are minimized. Such technology has powerful implications for genomic and proteomic studies, whereby large numbers of single cells are lysed, and subsequent chemical tests are all performed on the same chip [62–67]. Similar systems are used to perform analysis of $\backsim$ 15,000 chromosomes and proteins within a single experiment [66]. Such microfluidic devices also have great potential for massive parallelized and automated cell culture, for example, as demonstrated by an automatic 96-well microfluidic device for cell culture [35]. Such technology can also be applied for more detailed studies of individual cells: encapsulating individual cells in such nanoliter-scale compartments enables detection of compounds secreted by cells, and reveals the quantal nature of gene expression in cells [68].

4 Using flow to deform cells

The ability of cells to deform through narrow gaps and tortuous pathways is critical for many biological processes: cells are required to perfuse through capillaries of dimensions 2–15 μm [69]; undergo transendothelial migration through interstitial spaces that are no more than 2–3 μm; and migrate through tissue, including through the extracellular matrix that has pore sizes ranging from 0.1–10 μm. In circulating through the vasculature, the mechanical properties of blood cells and hydrogel particles are critical, determining both the time required for them to circulate, as well as which

organs they end up in [3,70–72]. Characterizing cell and nuclear deformability is thus critical to advance our understanding of cell retention, migration, and the spread of cancer: cancer cells show reproducible viscoelastic changes that correlate with malignant transformation [73,74]. Conventional methods to probe mechanical properties of cells or nuclei involve applying forces to cells and measuring the resulting response to derive details about the elastic and viscous moduli of the cell. While techniques such as micropipette aspiration [75], atomic force microscopy [76], and magnetic twisting cytometry [77], enable deforming cells with forces ranging from pN to μN, these techniques are time-consuming and therefore limited to small sample numbers: measurement rates are limited to no more than one cell per minute, with typical sample sizes of 10–100 cells. Microfluidic devices considerably improve the rates for mechanical characterization of cell populations, enabling population heterogeneity to be investigated. Most current microfluidic methods do not enable measurements of physical parameters, such as elastic or viscous moduli, but such qualitative investigations are revealing important differences between cell types.

4.1 Probing cell deformability by flow through micron-scale constrictions

The majority of microfluidic mechanical detection systems are based on the principle that softer, more deformable cells passage through a constriction faster than stiff cells [78,79]. This idea directly descends from bulk filtration assays that were developed in the past decades [3,80], and which are common in clinical use today [81–83]. There are two main advantages of emerging microfluidic methods over traditional bulk filtration methods: 1) soft lithography enables constrictions with precisely defined geometries to be fabricated; and 2) the passage time and morphology of each individual cell can be directly measured because the device is planar and optically transparent.

Cell deformation studies using microfluidic devices have been applied to a variety of cell types: acute lymphoblastic and acute myeloid leukemia (ALL and AML) cells [84,85]; breast epithelial cells (MCF-10A) and cancerous breast cells (MCF-7) [86]; as well as red blood cells in the context of malaria (*Plasmodium falciparum* infected cells) [87,88] and sickle cell disease [11]. All systems use a branched channel design system so that multiple constricted channels can be observed in parallel. By integrating additional features into planar designs, richer data sets can be obtained. For instance, marked changes in red blood cell mechanical properties are implicated in sickle cell anemia, which are mediated by oxygen and carbon monoxide levels in the blood. By smartly integrating a gaseous flow layer in proximity to the blood flow layer in a multilayer, gas-permeable PDMS devices enable direct observations of the effect of oxygen and carbon monoxide on occlusion in blood vessels [11]. Flowing cells through simple constricted entries of microchannels reveals that chemotherapy drugs increase the stiffness of leukemia cells [85]. With the ability to measure large numbers of >100 single cells, such methods also reveal skewed distribution of transit times, suggesting heterogeneity in cell mechanical properties [84]. The origins of such variability remain to be elucidated, but such single cell analyses highlights an important direction for determining specific treatments that target a particular subset of cells. Building on this concept, the ‘Cell Deformer’ device design better recapitulates this tortuous physiological trajectory–the pulmonary capillary bed has 50–100 constricted segments [89,90], thus cells typically passage through not one but multiple constrictions under physiological flow. Flowing cells through a series of constrictions thus enables measurements of both deformability and subsequent relaxation of individual cells (Fig. 5a). These studies also reveal the contributions of the cell nucleus to whole cell deformability (Rowat, in preparation).

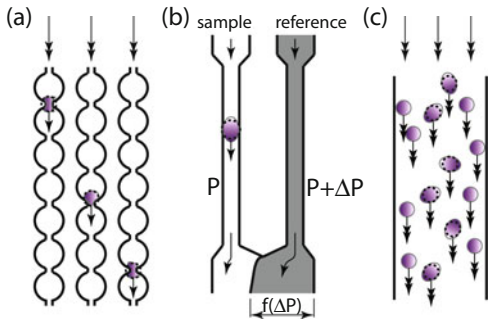

Fig. 5. Microfluidic devices to probe cell deformability. (a) The passage time for a cell to traverse a series of constrictions is used to differentiate the deformability of two cell populations. Arrows denote flow vectors and dashed black lines show deformed cells. (b) To measure the properties of deformed cells, a differential manometer exploits the pressure drop that occurs over a constricted channel, and manifests in the interfacial position between two fluid streams. (c) Inertial flow is used to probe cell deformability: at high flow rates, the more deformable cells migrate to the center of the channel.

4.2 Determining cell deformability by hydrodynamic resistance variations

As a cell flows through a constricted channel, it blocks the cross-sectional area of the channel and results in an increased hydrodynamic resistance. The high-speed microfluidic differential manometer system is designed to obtain precise measurements of this change in hydrodynamic resistance which depends on cell physical properties [91]. In this device, two identical $5 \times 5\,\mu\text{m}^2$ microchannels are fabricated in parallel: one is the sample channel through which cells in their carrier fluid flow; the other channel is the reference channel through which a dyed fluid flows at a controlled pressure. When cells passage through the sample channel and increase the channel resistance, the sample fluid flow rate decreases; this results in a differential pressure drop across the sample and reference channel; and a pressure-drop at the sample channel results in a lateral shift of the fluid–fluid interface (Fig. 5b). By relating the spatial variation of the fluid-fluid interface, Δx, to a calibrated $\Delta x - \Delta P$ relation, the absolute pressure drop can be obtained. Using this method, larger pressure drops are observed during passage of red blood cells with increased rigidity induced by glutaraldehyde treatment as compared to untreated control cells [91].

4.3 Deforming cells by inertial flow

Cell deformability can also be probed using inertial flow: at high flow rates, cells are subject to a fluid shear gradient that drives them laterally towards the channel walls, while competing wall-effect forces propel cells towards the channel center; the balance between these opposing forces determines their lateral position in the channel. Since more deformable cells migrate towards the channel center due to shape changes that alter the cell/fluid interface, a cell's lateral position can be used as a measure of its deformability (Fig. 5c). Exploiting this dependence of cell deformability on lateral position, subpopulations of cells within a heterogeneous population can be probed and isolated [27]. For example, more deformable, highly invasive cancerous cells preferentially travel along the channel center as compared to less invasive cancer cells. Given the flow rates necessary to operate these devices in the inertial regime, cells are rapidly characterized ($\backsim 22{,}000$ cells min^{-1}) [27]; they can also be passively separated by directing laterally segregated cell subpopulations to flow into separate

outlets. Such high throughput rates are a significant improvement over conventional methods to characterize cell mechanical properties.

5 Summary and outlook

Microfluidic methods continue to emerge as an important technology in biological research; the beauty of using flow is that large numbers of cells can be passively manipulated, making such methods very effective at characterizing large populations of individual cells. Exploiting flow to probe the biochemical and mechanical properties at the single cell level has already yielded important insights into the behavior of individual cells, as well as potential breakthroughs in medical and industrial applications such as single cell genotyping, sequencing, and directed evolution of enzymes. While some microfluidic devices can successfully operate with ultra-high throughput capacity, there are challenges that remain in increasing throughput, such as interfacing the microscale to the macroscale, optimizing data handling, and post-measurement analysis. Integrating mechanical, optical, electrical, and chemical stimulation and detection within microfluidic channels should contribute to the development of more automated devices. Such capabilities are essential to fully exploit the use of flow in probing single cells for basic and applied research that will further advance our understanding of cellular physiology and disease, as well as applications with social impact in health, medicine, and the environment.

The authors would like to acknowledge Prof. Dino Di Carlo and Dr. Lucas Frenz for their insightful comments during the preparation of this manuscript.

References

1. R. Skalak, P.I. Branemark, Science **164**, 717 (1969)
2. R.T. Yen, Y.C. Fung, Am. J. Physiol. **235**, H251 (1978)
3. G.P. Downey, G.S. Worthen, J. Appl. Physiol. **65**, 1861 (1988)
4. J.A. Rogers, R.G. Nuzzo, Materials Today **8**, 50 (2005)
5. D.C. Duffy, J.C. McDonald, O.J.A. Schueller, G.M. Whitesides, Anal. Chem. **70**, 4974 (1998)
6. J.C. McDonald, D.C. Duffy, J.R. Anderson, D.T. Chiu, H. Wu, O.J. Schueller, G.M. Whitesides, Electrophoresis **21**, 27 (2000)
7. M.C. Cole, P.J. Kenis, Sensors and Actuators B: Chemical **136**, 350 (2009)
8. L. Sohn, O. Saleh, G. Facer, A. Beavis, R. Allan, D. Notterman, Proc. National Acad. Sci. **97**, 10687 (2000)
9. J.J. Agresti, E. Antipov, A.R. Abate, K. Ahn, A.C. Rowat, J.C. Baret, M. Marquez, A.M. Klibanov, A.D. Griffiths, D.A. Weitz, Proc. National Acad. Sci. **107** (2010)
10. J. Guck, S. Schinkinger, B. Lincoln, F. Wottawah, S. Ebert, M. Romeyke, D. Lenz, H.M. Erickson, R. Ananthakrishnan, D. Mitchell, et al., Biophys. J. **88**, 3689 (2005)
11. J.M. Higgins, D.T. Eddington, S.N. Bhatia, L. Mahadevan, Proc. Natl. Acad. Sci. USA **104**, 20496 (2007)
12. A. Siegel, D. Bruzewicz, D. Weibel, G.M. Whitesides, Adv. Mater. **19**, 727 (2007)
13. J. Melin, S. Quake, Annu. Rev. Biophys. Biomol. Struct. **36**, 213 (2007)
14. M.A. Unger, H.P. Chou, T. Thorsen, A. Scherer, S.A. Quake, Science **288**, 113 (2000)
15. A.R. Abate, J.J. Agresti, D.A. Weitz, Appl. Phys. Lett. **96**, 203509 (2010)
16. H. Bruus, *Theoretical Microfluidics* (Oxford University Press, Oxford, 2008)
17. H.A. Stone, A. Stroock, A. Ajdari, Ann. Rev. Fluid Mech. **36**, 381 (2004)
18. T. Squires, S.R. Quake, Rev. Modern Physics **77**, 977 (2005)
19. E. Lucchetta, J. Lee, L. Fu, N. Patel, R. Ismagilov, Nature **434**, 1134 (2005)
20. F. Balagaddé, L. You, C.L. Hansen, F.H. Arnold, S.R. Quake, Science **309**, 137 (2005)

21. J. Ryley, O. Pereira-Smith, Yeast **23**, 14 (2006)
22. D. Di Carlo, L.Y. Wu, L.P. Lee, Lab on a Chip **6**, 1445 (2006)
23. S. Nagrath, L.V. Sequist, S. Maheswaran, D.W. Bell, D. Irimia, L. Ulkus, M.R. Smith, E.L. Kwak, S. Digumarthy, A. Muzikansky, et al., Nature **450**, 1235 (2007)
24. S.C. Hur, A.J. Mach, D. Di Carlo, Biomicrofluidics **5**, 022206 (2011)
25. D. Di Carlo, Lab on a Chip **9**, 3038 (2009)
26. D. Di Carlo, D. Irimia, R.G. Tompkins, M. Toner, Proc. National Acad. Sci. **104**, 18892 (2007)
27. S. Hur, N. Henderson-MacLennan, E. McCabe, D. Di Carlo, Lab on a Chip **11**, 912 (2011)
28. Z. Wu, B. Willing, J. Bjerketorp, J.K. Jansson, L. Hjort, Lab on a Chip **9**, 1193 (2009)
29. E.S. Asmolov, A.A. Osiptsov, Phys. Fluids **21**, 063301 (2009)
30. S. Kuntaegowdanahalli, A. Bhagat, G. Kumar, I. Papautsky, Lab on a Chip **9**, 2973 (2009)
31. H.A. Nieuwstadt, R. Seda, D.S. Li, J.B. Fowlkes, J.L. Bull, Biomedical Microdevices **13**, 97 (2011)
32. Y.S. Choi, K.W. Seo, S.J. Lee, Lab on a Chip **11**, 460 (2011)
33. C.A. Stan, L. Guglielmini, A.K. Ellerbee, D. Caviezel, H.A. Stone, G.M. Whitesides, Phys. Rev. E **84**, 036302 (2011)
34. A.C. Rowat, J. Bird, J.J. Agresti, O.J. Rando, D.A. Weitz, Proc. Natl. Acad. Sci. USA **106**, 18149 (2009)
35. R. Gómez-Sjöberg, A.A. Leyrat, D.M. Pirone, C.S. Chen, S.R. Quake, Analytical Chem. **79**, 8557 (2007)
36. S. Anna, N. Bontoux, H. Stone, Appl. Phys. Lett. **82**, 364 (2003)
37. J. Guck, R. Ananthakrishnan, H. Mahmood, T. Moon, C. Cunningham, J. Ks, Biophys. J. **81**, 767 (2001)
38. T.W. Remmerbach, F. Wattawah, J. Dietrich, B. Lincoln, C. Wittekind, J. Guck, Cancer Res. **69**, 1728 (2009)
39. J. Guck, R. Ananthakrishnan, T. Moon, C. Cunningham, J. Ks, Phys. Rev. Lett. **84**, 5451 (2000)
40. Y.B. Lu, K. Franze, G. Seifert, C. Steinhuser, F. Kirchhoff, H. Wolburg, J. Guck, P. Janmey, E.Q. Wei, J. Ks, et al., Proc. National Acad. Sci. **103**, 17759 (2006)
41. S.S. Shevkoplyas, T. Yoshida, L.L. Munn, M.W. Bitensky, Analytical Chem. **77**, 933 (2005)
42. G. Charvin, F.R. Cross, E.D. Siggia, PLoS one **3**, e1468 (2008)
43. S. Cookson, N. Ostroff, W.L. Pang, D. Volfson, J. Hasty, Mol. Syst. Biol. **1**, 0024 (2005)
44. N. Balaban, J. Merrin, R. Chait, L. Kowalik, S. Leibler, Science **305**, 1622 (2004)
45. E. Pratt, C. Huang, B. Hawkins, J. Gleghorn, B. Kirby, Chem. Eng. Sci. **66**, 1508 (2011)
46. S.J. Tan, L. Yobas, G.Y.H. Lee, C.N. Ong, C.T. Lim, Biomedical Microdevices **11**, 883 (2009)
47. A.M. Skelley, O. Kirak, H. Suh, R. Jaenisch, J. Voldman, Nat. Meth. **6**, 147 (2009)
48. A.D. Stroock, S.K. Dertinger, A. Ajdari, I. Mezic, H.A. Stone, G.M. Whitesides, Science **295**, 647 (2002)
49. S.L. Stott, C.H. Hsu, D.I. Tsukrov, M. Yu, D.T. Miyamoto, B.A. Waltman, S.M. Rothenberg, A.M. Shah, M.E. Smas, G.K. Korir, et al., Proc. National Acad. Sci. **107**, 18392 (2010)
50. N.L. Jeon, S.K. Dertinger, D.T. Chiu, I.S. Choi, A.D. Stroock, G.M. Whitesides, Langmuir **16**, 8311 (2000)
51. K.R. King, S. Wang, A. Jayaraman, M.L. Yarmush, M. Toner, Lab on a Chip **8**, 107 (2008)
52. S. Paliwal, P.A. Iglesias, K. Campbell, Z. Hilioti, A. Groisman, A. Levchenko, Nature **446**, 46 (2007)
53. M. Skoge, M. Adler, A. Groisman, H. Levine, W.F. Loomis, W.J. Rappel, Integrative Biol. **2**, 659 (2010)
54. O. Amadi, M. Steinhauser, Y. Nishi, S. Chung, R. Kamm, A. McMahon, R. Lee, Biomedical Microdevices **12**, 1027 (2010)

55. C. Holtze, A.C. Rowat, J.J. Agresti, J.B. Hutchison, F.E. Angile, C.H.J. Schmitz, S. Koster, H. Duan, K.J. Humphry, R.A. Scanga, et al., Lab on a Chip **8**, 1632 (2008)
56. J.F. Edd, D. Di Carlo, K.J. Humphry, S. Köster, D. Irimia, D.A. Weitz, M. Toner, Lab on a Chip **8**, 1262 (2008)
57. J.C. Baret, O.J. Miller, V. Taly, M. Ryckelynck, A. El-Harrak, L. Frenz, C. Rick, M.L. Samuels, J.B. Hutchison, J.J. Agresti, et al., Lab on a Chip **9**, 1850 (2009)
58. D.R. Link, S.L. Anna, D.A. Weitz, H.A. Stone, Phys. Rev. Lett. **92**, 054503 (2004)
59. A.R. Abate, T. Hung, P. Mary, J.J. Agresti, D.A. Weitz, Proc. Natl. Acad. Sci. USA **107**, 19163 (2010)
60. C. Schmitz, A.C. Rowat, S. Köster, D.A. Weitz, Lab on a Chip **9**, 44 (2009)
61. C. Schmitz, A.C. Rowat, S. Koester, J.J. Agresti, D.A. Weitz, *Microfluidic device for storage and well-defined arrangement of droplets*, Patent No. WO/2009/134395 (2009)
62. J.F. Zhong, Y. Chen, J.S. Marcus, A. Scherer, S.R. Quake, C.R. Taylor, L.P. Weiner, Lab on a Chip **68**, 68 (2008)
63. P.C. Blainey, A.C. Mosier, A. Potanina, C.A. Francis, S.R. Quake, PLoS One **6**, e16626 (2011)
64. H.C. Fan, J. Wang, A. Potanina, S.R. Quake, Nature Biotechnol. **29**, 51 (2011)
65. S.J. Maerkl, S.R. Quake, Science **315**, 233 (2007)
66. D. Gerber, S.J. Maerkl, S.R. Quake, Nat. Meth. **6**, 71 (2009)
67. D. Pushkarev, N.F. Neff, S.R. Quake, Nat. Biotechnol. **27**, 847 (2009)
68. L. Cai, N. Friedman, X. Xie, Nature **440**, 358 (2006)
69. C. Doerschuk, N. Beyers, H. Coxson, B. Wiggs, J. Hogg, J. Appl. Physiol. **74**, 3040 (1993)
70. T. Merkel, S. Jones, K. Herlihy, F. Kersey, A. Shields, M. Napier, J. Luft, H. Wu, W. Zamboni, A. Wang, et al., Proc. Natl. Acad. Sci. USA **108**, 586 (2011)
71. M. Diez-Silva, M. Dao, J. Han, C.T. Lim, S. Suresh, MRS Bull. **35**, 382 (2010)
72. C. Lim, A. Li, Theor. Appl. Mech. Lett. **1**, 014000 (2011)
73. S. Suresh, Acta Biomater **3**, 413 (2007)
74. M. Teitell, S. Kalim, J. Schmit, J. Reed, *Biomechanics of Single Cells and Cell Populations* (Springer, US, 2010), p. 235
75. X. Liu, Y. Wang, Y. Sun, *Real-time high-accuracy micropipette aspiration for characterizing mechanical properties of biological cells*, in *IEEE International Conference on Robotics and Automation* (Roma, Italy, 2007), p. 1930
76. C. Franz, P.H. Puech, Cell. Molec. Bioengineering **1**, 289 (2008)
77. B. Fabry, G. Maksym, R. Hubmayr, J. Butler, J. Fredberg, J. Magnet. Magnet. Mater. **194**, 120 (1999)
78. H. Wyss, T. Franke, E. Mele, D. Weitz, Soft Matter **6**, 4550 (2010)
79. M.A. Tsai, R. Waugh, P. Keng, Biophys. J. **74**, 3282 (1998)
80. G.S. Worthen, r. Schwab, B., E.L. Elson, G.P. Downey, Science **245**, 183 (1989)
81. G. Nash, Biorheology **27**, 872 (1990)
82. S. Svenmarker, E. Jansson, Perfusion **15**, 33 (2000)
83. L.A. Kirschenbaum, M. Aziz, M.E. Astiz, D.C. Saha, E.C. Rackow, Am. J. Respiratory Critical Care Med. **161**, 1602 (2000)
84. M. Rosenbluth, W. Lam, D. Fletcher, Lab. Chip. **8**, 1062 (2008)
85. W.A. Lam, M.J. Rosenbluth, D.A. Fletcher, Blood **109**, 3505 (2007)
86. H. Hou, Q.S. Li, G.Y.H. Lee, A.P. Kumar, C.N. Ong, C.T. Lim, Biomedical Microdevices **11**, 557 (2009)
87. H. Bow, I.V. Pivkin, M. Diez-Silva, S.J. Goldfless, M. Dao, J.C. Niles, S. Suresh, J. Han, Lab on a Chip **11**, 1065 (2011)
88. T. Herricks, M. Antia, P.K. Rathod, Cellular Microbiol. **11**, 1340 (2009)
89. J. Hogg, Physiol. Rev. **67**, 1249 (1987)
90. J. Hogg, H. Coxson, M. Brumwell, N. Beyers, C. Doerschuk, W. MacNee, B. Wiggs, J. Appl. Physiol. **77**, 1795 (1994)
91. M. Abkarian, M. Faivre, H.A. Stone, Proc. Natl. Acad. Sci. USA **103**, 538 (2006)